

KINETICS AND CLUSTERING OF DUST PARTICLES IN SUPERSONIC TURBULENCE WITH SELF-GRAVITY

Robert Hedvall¹ and Lars Mattsson²

¹*Department of Physics, Stockholm University, Stockholm, Sweden*

²*Nordita, KTH Royal Institute of Technology & Stockholm University, Stockholm, Sweden*

Keywords: hydrodynamics — turbulence — ISM: dust, extinction

HYDRODYNAMIC SIMULATIONS WITH PARTICLES

We present a simulation of isothermal supersonic (rms Mach number $\mathcal{M}_{\text{rms}} \sim 3$) turbulent gas with inertial particles (dust) and self-gravity in statistical steady-state (S3G), which we compare with a corresponding simulation without self-gravity (S3), similar to those in [Mattsson et al. \(2019\)](#). The computational domains are 3D boxes (512^3) with periodic boundaries and sides of equal length $L = 2\pi$, where we solve the compressible Navier-Stokes equations with stochastic forcing. We use the PENCIL CODE, a high-order finite difference code capable of simulating compressible flows with inertial particles ([Brandenburg & Dobler 2002](#)).

The gas flow is characterized by the density ρ and the flow velocity \mathbf{u} . Dust-particle velocities \mathbf{v}_i are followed using a Lagrangian equation of motion (EOM) for each particle i (10^7 discrete inertial particles in 10 size bins with 10^6 particles). Grain-sizes are characterized by $\alpha = (\rho_{\text{gr}}/\langle\rho\rangle)(a/L)$, where a is the grain radius and ρ_{gr} is the bulk material density ([Hopkins & Lee 2016](#)). Without self-gravity, the simulation can thus be scaled arbitrarily. S3G, however, is not scale-free. It is in steady state, but close to gravitationally unstable, since we adopt a *Jeans wavelength*, $\lambda_J = 2\pi = L$, which provides the strongest influence of gravity on the dynamics of gas and dust without causing irreversible gravitational collapses.

RESULTS AND DIRECTIONS FOR FURTHER STUDY

Mean velocities and clustering

Clustering of particles can be quantified by their first nearest neighbor distance (1-NND) ([Monchaux et al. 2012](#)). We compare the measured average 1-NND $\langle r_{\text{obs}} \rangle$ to that expected from a random isotropic distribution $\langle r_{\text{exp}} \rangle$. This average nearest neighbor ratio, $R_{\text{ANN}} = \langle r_{\text{obs}} \rangle / \langle r_{\text{exp}} \rangle$, is $R_{\text{ANN}} \approx 1$ for unclustered grains. If $R_{\text{ANN}} < 1$ the particles are clustered, since the average 1-NND is lower. We must distinguish between *compaction* and *fractal* clustering, where the latter is due to rotation of the flow rather than compression. Fractal clustering is usually measured by the correlation dimension $d_2 = \lim_{\delta r \rightarrow 0} \{\ln[\langle \mathcal{N}(\delta r) \rangle] / \ln \delta r\}$, where \mathcal{N} is the expected number of particles inside a ball of radius δr surrounding a test particle at the centre of the ball.

Fig. 1 (lower left) shows that root-mean-square (rms) grain velocities depend on particle size, since lighter particles couple better to the gas due to lower inertia than heavier particles. R_{ANN} and d_2 (Fig. 1, left panels) are also determined by particle size, except for $\alpha = 8.0, 16.0$. Particles coupled to a turbulent gas will experience a higher degree of fractal clustering (low d_2) since they get temporarily trapped in vortices and may therefore accumulate in convergence zones in between vortices as they are being expelled ([Mattsson et al. 2019](#)).

The influence of gravity

Comparing S3G and S3, we find that self-gravity does not cause any significant increase in clustering, as determined by R_{ANN} and the correlation dimension (d_2), regardless of particle size (Fig. 1, upper panels). However, there is a brief initial phase of strong clustering for $\alpha = 8.0, 16.0$ in both simulations, but much more prominent in S3G where particles are also gravitationally accelerated. With more inertia, and thus less affected by drag, heavier particles free-fall and cluster faster than lighter particles coupling to the turbulent gas.

When a steady state is reached, v_{rms} is a function of α , which can be derived from the EOM,

$$\frac{d\mathbf{v}_i}{dt} = \frac{\mathbf{u} - \mathbf{v}_i}{\tau_{s,i}} - \nabla\Phi, \quad (1)$$

where Φ is the gravitational potential and the stopping time $\tau_{s,i}$, defining the coupling efficiency between gas and dust particles, is given by (Draine & Salpeter 1979),

$$\tau_{s,i} = \sqrt{\frac{\pi \rho_{\text{gr}} a}{8 \rho c_s}} \left(1 + \frac{9\pi |\mathbf{v}_i - \mathbf{u}|^2}{64 c_s^2} \right)^{-1/2}. \quad (2)$$

Note that $\tau_{s,i} \propto \alpha$ explains why there is no significant change in velocities for the small particles (kinetic drag dominates). Fig. 1 (lower left) shows that only heavy particles ($\alpha = 8.0, 16.0$) show elevated v_{rms} in the presence of self-gravity and the speed distributions (lower right) are significantly affected for $\alpha = 8.0, 16.0$ (distributions are shifted to higher values in S3G compared to S3). For $\alpha = 8.0$ the rms-velocity increases from $v_{\text{rms}}/c_s = 0.52$ to 0.84 (62%) and for $\alpha = 16.0$, $v_{\text{rms}}/c_s = 0.33$ rises to 0.83 (152%).

The stopping time $\tau_{s,i} \propto \alpha$ differs by a factor of ~ 160 between the smallest and the largest particles. Acceleration due to gravity becomes the dominant force for sufficiently large particles, which explains the discrepancies seen in Fig. 1. To describe the difference in velocities between S3G and S3, we note that v_{rms} satisfies a relation $v_{\text{rms}}^2/u_{\text{rms}}^2 = 1 - \Psi(\alpha)$, with $\Psi = \langle (\mathbf{u} + \mathbf{v}_i) \cdot (\mathbf{u} - \mathbf{v}_i) \rangle / \langle \mathbf{u} \cdot \mathbf{u} \rangle$. Assuming $\tau_{s,i}$ is a function of α only, (1) and statistical steady-state yields,

$$\Psi = \frac{\tau_{s,i}^2}{u_{\text{rms}}^2} \left(\left\langle \frac{d\mathbf{v}_i}{dt} \cdot \frac{d\mathbf{v}_i}{dt} \right\rangle - \langle \nabla\Phi \cdot \nabla\Phi \rangle \right), \quad (3)$$

where terms within brackets are squares of the rms values of total and gravitational acceleration (a_{rms} and g_{rms} , respectively). First, we note that in the tracer-particle limit (very small grains; $v_i \rightarrow \mathbf{u}$), $\Psi = 0$. Second, for larger particles, v_{rms} as a function of α must reach a minimum and then rise again because $g_{\text{rms}} = \text{constant}$ and a_{rms} must be a bounded function of α . Thus, Ψ must also be a bounded function. For large grains, $\tau_{s,i}$, as in (2), is actually limited by $|\mathbf{u} - \mathbf{v}|/c_s$ and Ψ will approach an arbitrary finite value as $\tau_{s,i} a_{\text{rms}}/\tau_{s,i} g_{\text{rms}}$ approaches its upper limit. Obviously, \mathcal{M}_{rms} plays a role here and for $\mathcal{M}_{\text{rms}} \sim 1$ simple scalings suggest that v_{rms} reaches its minimum for $\alpha \sim 1$ and approach a finite value for really large grains, possibly exceeding u_{rms} . More and extended simulations will likely confirm or disprove this idea.

REFERENCES

- | | |
|---|--|
| <p>Brandenburg, A., & Dobler, W. 2002, <i>Computer Physics Communications</i>, 147, 471</p> <p>Draine, B. T., & Salpeter, E. E. 1979, <i>ApJ</i>, 231, 438</p> <p>Hopkins, P. F., & Lee, H. 2016, <i>MNRAS</i>, 456, 4174</p> | <p>Mattsson, L., Bhatnagar, A., Gent, F. A., & Villarroel, B. 2019, <i>MNRAS</i>, 483, 5623</p> <p>Monchaux, R., Bourgoin, M., & Cartellier, A. 2012, <i>International Journal of Multiphase Flow</i>, 40, 1</p> |
|---|--|

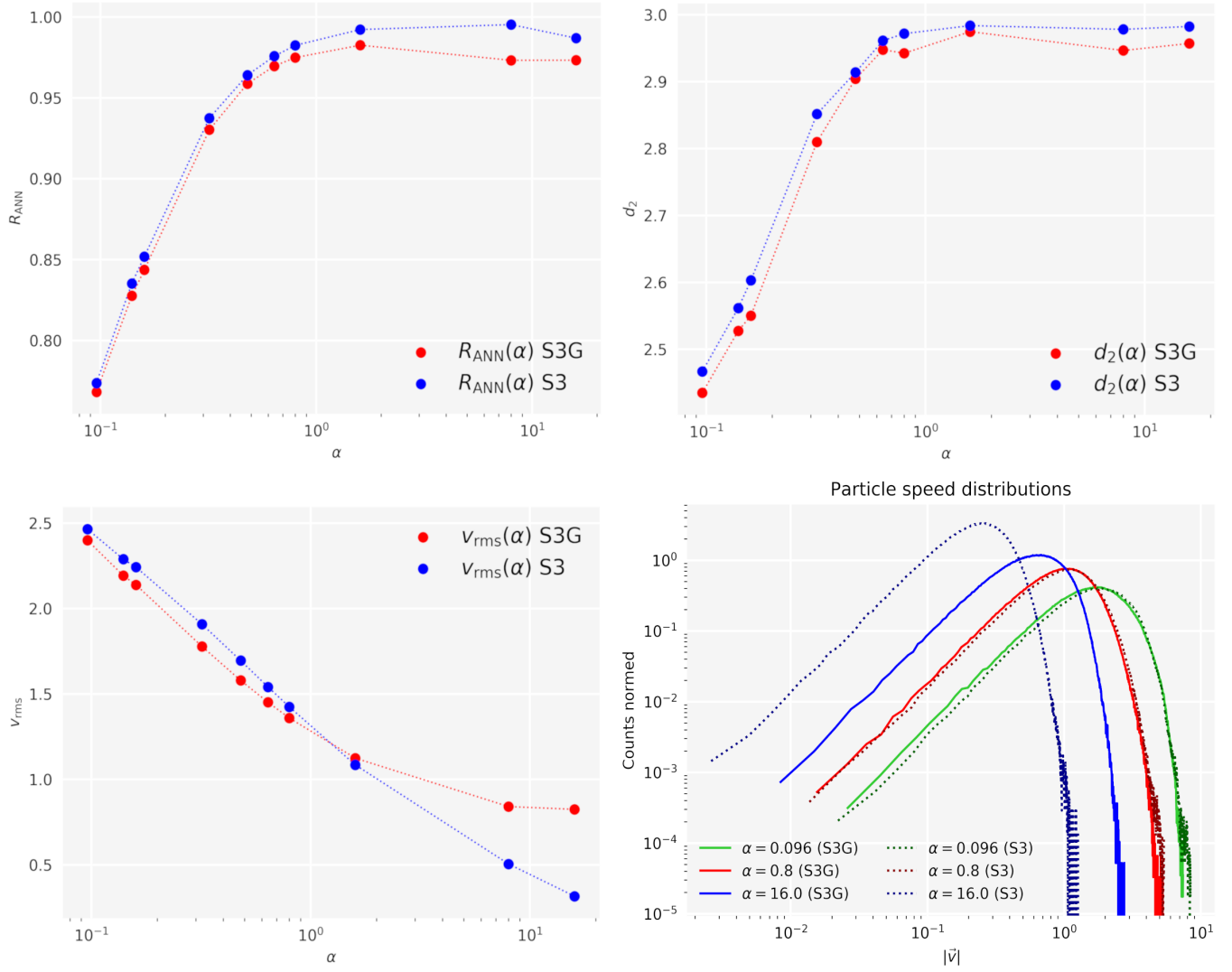


Figure 1. Comparison of simulations. *Top:* R_{ANN} and d_2 as functions of α . *Bottom:* v_{rms} in units of c_s as function of α and speed distributions for different α .